How Does Protein Architecture Facilitate the Transduction of ATP Chemical-Bond Energy into Mechanical Work? The Cases of Nitrogenase and ATP Binding-Cassette Proteins

Jie-Lou Liao and David N. Beratan
Departments of Chemistry and Biochemistry, Duke University, Durham, North Carolina

ABSTRACT Transduction of adenosine triphosphate (ATP) chemical-bond energy into work to drive large-scale conformational changes is common in proteins. Two specific examples of ATP-utilizing proteins are the nitrogenase iron protein and the ATP binding-cassette transporter protein, BtuCD. Nitrogenase catalyzes biological nitrogen fixation whereas BtuCD transports vitamin B_{12} across membranes. Both proteins drive their reactions with ATP. To interpret how the mechanical force generated by ATP binding and hydrolysis is propagated in these proteins, a coarse-grained elastic network model is employed. The analysis shows that subunits of the proteins move against each other in a concerted manner. The lowest-frequency modes of the nitrogenase iron protein and of the ATP binding-cassette transporter BtuCD protein are found to link the functionally critical domains, and these modes are suggested to be responsible for (at least the initial stages) large-scale ATP-coupled conformational changes.

INTRODUCTION

Protein machines convert the free energy of adenosine triphosphate (ATP) binding and hydrolysis into work. ATP-utilizing biomolecular machines drive muscle contraction, bacterial locomotion, cell division, intercellular and intracellular transport, and genome transcription, for example (Hill, 1977; Cramer and Knaff, 1989). Our goal is to understand some of the minimal constraints on structure and dynamics for functioning ATP-driven protein machines. As prototypes, we examine two molecular machines, nitrogenase and the ATP binding-cassette vitamin B_{12} transporter, BtuCD.

Biological nitrogen fixation catalyzed by the enzyme nitrogenase produces more than 60% of the world's annual supply of new ammonia (Schlesinger, l991). Nitrogenase consists of two metalloproteins, a 64 kDa iron protein (Fe protein) and a 240 kDa molybdenum protein (MoFe protein) (Einsle et al., 2002; Howard and Rees, 1996; Eady, 1996). The Fe protein is a dimer with a single [4Fe4S] cluster linking the two subunits. The MoFe protein is an $\alpha_2\beta_2$ tetramer that contains an iron-sulfur P-cluster, presumably the intermediate electron acceptor, and the catalytic nitrogen-reducing MoFe cofactor. The Fe protein delivers electrons to the MoFe protein in a transient complex triggered by ATP binding to the Fe protein.

The binding and hydrolysis of ATP, which is required for nitrogen fixation, changes the iron-protein conformation and is coupled to protein-protein binding. Binding ATP triggers substantial changes in the protein environment near the [4Fe4S] cluster (Schindelin et al., 1992), despite >15 Å distance between the edges of the ATP binding sites and the [4Fe4S] cluster. Experimental studies (Stephens et al., l996; Jang et al., 2000a) show ATP binding and protein-protein association leads to a lowering in the midpoint potential of the [4Fe4S] cluster, enhancing the driving force for electron transfer. Recent theoretical analysis (Kurnikov et al., 2002) suggests that the redox potential lowering in the [4Fe4S] cluster upon protein-protein binding results from cofactor desolvation.

The ATP binding-cassette (ABC) transporters are ubiquitous membrane proteins that couple ATP binding and hydrolysis to the translocation of substrates, including amino acids, peptides, ions, sugars, toxins, lipids, and drugs across membranes. Multidrug resistance is responsible for up to 60% of all hospital-acquired infections globally (WHO, 2000; Chang and Roth, 2001) and is associated with ABC transporters. Structural studies indicate that ABC transporters invariably contain two domains, a transmembrane (TM) binding domain, and a nucleotide-binding domain (i.e., ATP binding cassette). The transmembrane domain plays a primary role in recognizing and transporting substrates through the lipid bilayer. After the substrate is bound and transported across the membrane, the ABC transporter protein returns to its initial state. The ATP binding and hydrolysis drives the cycle. The ABC transporter proteins have a number of highly conserved ABC cassette motifs. The ATP binding and hydrolysis in ABC proteins couple to substantial conformational changes, such as the opening or closing of the chamber formed by the transmembrane domains. These openings are $\sim$25 Å wide in the transmembrane direction in *E. coli* MsbA, for example (Chang and Roth, 2001). This large-scale conformational change is apparently related to unidirectional substrate translocation.

In recent years, considerable progress has been made in elucidating the structure of ABC transporters (Hung et al.,

Submitted December 17, 2003, and accepted for publication April 2, 2004.

Address reprint requests to Prof. David N. Beratan, Duke University, Dept. of Chemistry, 228C Gross Chem., Durham, NC 27708-0346. Tel.: 919-660-1526; E-mail: david.beratan@duke.edu.

0006-3495/04/08/1369/09 $2.00

doi: 10.1529/biophysj.103.038653

1998; Rosenberg et al., 2001; Yuan et al., 2001; Chang and Roth, 2001; Locher et al., 2002). Recently, a molecular dynamics (MD) simulation of the ABC nucleotide-binding domain was performed to identify hinges and switches of the nucleotide-binding domain conformational change and subunit-subunit interfaces (Jones and George, 2002). All of these studies suggest that the ABC transporters use a common mechanism to power the translocation of substrates across cell membranes (Locher et al., 2002; Chang and Roth, 2001). As an example, the BtuCD protein from *Escherichia coli* (Locher et al., 2002) is examined here. The ABC transporter BtuCD is a homodimer that mediates vitamin B_{12} uptake.

Despite the diversity in the function of these two proteins, the nitrogenase Fe protein and the *E. coli* BtuCD both have a dimeric structure. The dimeric structure suggests ''lever arms'' that could generate large-scale conformational changes involving the relative movement of these structural domains. This sort of domain motion likely arises in a variety of protein machines, from catalysts to regulatory proteins (Mogilner et al., 2002).

It is generally thought that nitrogenase and ABC transporter mechanisms are similar to those of the general class of nucleotide-utilizing proteins (Schindelin et al., 1992; Jang et al., 2000a; Strop et al., 2001; Chang and Roth, 2001; Locher et al., 2002). In nucleotide-binding proteins, MgATP acts at a distance to induce protein conformational changes that drive biological processes including signal transduction, membrane and organelle transport, DNA replication, and muscle contraction. Studies of these two specific proteins may, therefore, be of more general relevance.

Although considerable progress has been made in interpreting nitrogenase and ABC transporter mechanisms, two intriguing functional questions remain:

1. How can the proteins move cooperatively in response to ATP binding (and hydrolysis)?
2. How do the proteins transmit the force generated by ATP binding to the functional domains at distances well beyond van der Waals contact (>15 Å) to drive large-scale conformational changes?

Protein motion, especially ATP-coupled motion, is highly anharmonic. Nevertheless, normal-mode analysis has been used successfully to provide qualitative and quantitative insights into protein structure and dynamics (Tama and Sanejouand, 2001). Normal-mode analysis (Li and Cui, 2002, 2004; Tama and Sanejouand, 2001) indicates that low-frequency modes are responsible for large-scale conformational changes. These modes are delocalized and can couple distant regions. In principle, the detailed dynamical behavior associated with large-scale conformational changes of proteins can be elucidated by combined molecular dynamics and normal-mode analysis (Tama and Sanejouand, 2001). However, all-atom MD approaches are not yet feasible for describing long timescale motion of these very large proteins (Karplus and McCammon, 2002). Coarse-grained models can be used to avoid some of the challenges associated with system size. Based on the finding that large-scale motion in proteins can be described approximately by using simple pairwise Hook's law potentials with a single spring-constant parameter (Tirion, 1996), the coarse-grained Gaussian network (GNM) (Bahar et al., 1997) and anisotropic network models (ANM) (Atilgan et al., 2002) were developed. In these models, the nodes of the network represent the amino acid residues, and the linkers are springs with a single spring constant connecting all nodes within a cutoff radius. As such, the fluctuations of the proteins around their equilibrium geometries are assumed to be Gaussian-distributed. Protein crystallographic B factors can be predicted well (Atilgan et al., 2002) with these harmonic methods. The GNM method assumes a one-dimensional chain and calculates the isotropic thermal-fluctuation amplitudes of amino acid residues (represented by their α-carbons), whereas its extension, ANM, is three-dimensional. These elastic network models (ENMs) have been widely used to analyze protein dynamics (Tirion, 1996; Bahar et al., 1997, 1999; Keskin et al., 2000, 2002; Doruker et al., 2000). Detailed studies indicate that both of these models capture key autocorrelation fluctuations in agreement with x-ray crystallographic data. Cross-correlations are also calculated consistently between the GNM and ANM methods (Bahar et al., 1997; Atilgan et al., 2002; Isin et al., 2002; Xu et al., 2003).

PROTEIN STRUCTURES

Nitrogenase iron protein

We focus first on the nitrogenase proteins from *Azotobacter vinelandii*, denoted *Av*. The structure and function of *Av* nitrogenase are similar to those of other species, including *Clostridium pasteurianum*. The free *Av* Fe protein (Av_2), shown in Fig. 1, binds ADP and is discussed in detail here since the conformation of the MoFe protein (Av_1) changes little upon Av_1–Av_2 binding (Schindelin et al., 1992; Schlessman et al., 1998; Jang et al., 2001a,b; Strop et al., 2001).

The Av_2 protein is a homodimer. Each monomer contains a mixed α/β-sheet polypeptide fold with an eight-strand β-sheet flanked by nine α-helices. A noncrystallographic twofold axis passes through the [4Fe4S] cluster and relates the two subunits in the Fe protein. The twisted β-sheet core of each subunit contains seven parallel strands and one short antiparallel strand, β_3, which is located at one edge of the β-sheet. The β-strand order is 3-4-2-5-1-6-7-8. Crystal structures indicate topological switch points formed by the loops at the C-terminal ends of several β-strands. The loops seem to create binding sites for ATP and cofactors, essential for Fe-protein function. For example, the loops following the β_1 and β_2 strands are associated with nucleotide binding (P-loop, see below), whereas the loops following β_5 and β_6 involve cysteine ligands to the [4Fe4S] cluster.

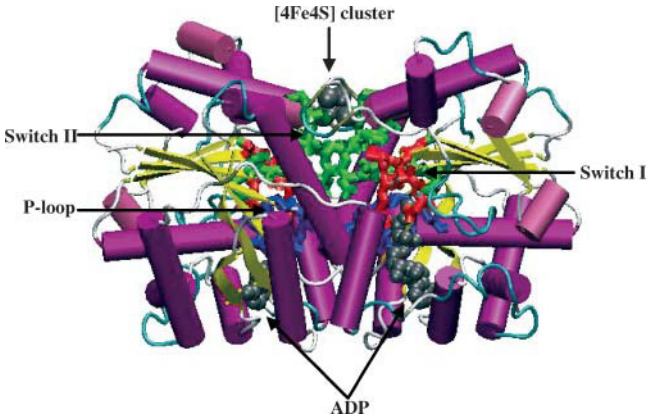

FIGURE 1 Structure of the nitrogenase Fe protein, Av_2. The α-helices are shown as purple cylinders and the β-strands are depicted as yellow ribbons. The P-loop, Switch I, and Switch II regions are displayed in blue, red, and green, respectively. The [4Fe4S] cluster and the ADP molecules are rendered using solid spheres. The crystallographic structure is from the PDB file 1Fe6P (Jang et al., 2000b).

The crystal structures of the Av_2 Fe protein indicate that there are three significant regions that may be related to the Av_2 protein conformational changes: 1), a phosphate-binding loop (P-loop), or so-called Walker A motif (Schlessman et al., 1998) containing the *G-X-X-X-G-K-S/T* (*X* means ''no consensus'') motif corresponding to 9–16 residues in Av_2; 2), a Switch I region located at the Fe-protein surface including residues 38–43, involved in interactions with the MoFe protein; and 3), a Switch II region consisting of residues from 125 to 135 (related to the conserved *D-X-X-G* sequence), in which Cys^{132} provides two of the four ligands to the [4Fe4S] cluster (Jang et al., 2000a). The crystal structures suggest that Switch I provides a mechanism for propagating the force generated from binding and hydrolysis of MgATP to the Fe-protein surface to control the protein-protein interaction (Jang et al., 2000b). The structure of Switch II suggests a mechanism for how nucleotide-binding couples to the [4Fe4S] cluster. The switch regions undergo conformational changes upon hydrolysis of nucleotide. The Fe protein displays structural similarity in these three regions to other nucleotide-binding proteins, including myosin and the G-protein *ras*. Therefore, investigations into the motion of these three regions in Av_2 may provide clues to energy transduction in other nucleotide-dependent proteins. In nitrogenase, the protein environment surrounding the [4Fe4S] cluster is of particular interest. The crystal structures (Schlessman et al., 1998) indicate that the [4Fe4S] cluster is buttressed on three sides by the main-chain atoms of residues 96–100 and 132–134, as well as by hydrophobic side chains of residues 98, 130, and 135. These invariant residues are likely critical for maintaining the appropriate cluster environment (Schlessman et al., 1998). The thiol ligands of Cys^{97} and Cys^{132} from each of the two Av_2 subunits coordinate the [4Fe4S] cluster (Schlessman et al., 1998).

BtuCD protein structure

The BtuCD structure from *E coli*, determined by x-ray crystallography (3.2 Å resolution) (Locher et al., 2002), is displayed in Fig. 2. The assembled complex of the BtuCD protein is 90 Å × 60 Å × 30 Å (Locher et al., 2002). Each subunit of the dimer contains a transmembrane domain and an ATP-binding domain (an ABC unit). The two transmembrane subunits and the two ABC units of the homodimer are designated BtuC and BtuD, respectively (Locher et al., 2002). A transmembrane domain contains 10 α-helices, denoted *TM1–TM10*. Among these helices, *TM4* (residues 114–138), *TM*5 (residues 142–166), and *TM10* (and their counterparts in the other subunit) are related to the large conformational rearrangements in the protein. The interface between the two transmembrane domains is constructed by *TM5* of one subunit and *TM10* of the other (and vice versa). These four α-helices define a cavity. This cavity is open to the periplasmic space and is closed to the cytoplasm by residues in *TM4* and *TM5,* referred to as a gate at the transporter center. The transmembrane domains provide a pathway for substrate transport through the lipid bilayers.

The nucleotide-binding domain includes a six-strand β-sheet surrounded by nine α-helices and a peripheral three-strand β-sheet. This domain contains a P-loop (Walker A), Walker B motif (including consensus sequence *hhhhD*; here *h* indicates a hydrophobic residue), ABC signature region, Q-loop, and switch region. The sequence comparison indicates that, like other ABC cassettes, residues critical to ATP binding are highly conserved. These residues involve those in the Walker-A/B motifs, a glutamine from the

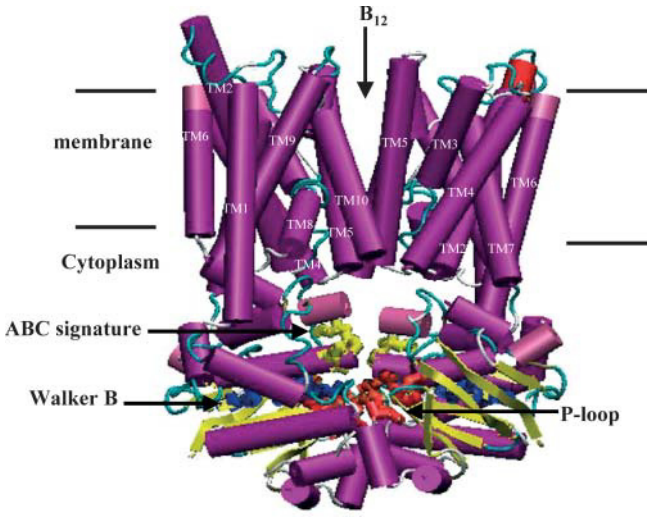

FIGURE 2 Structure of the ABC transporter, BtuCD. The α-helices are shown as purple cylinders and the β-strands are depicted as yellow ribbons. The P-loop, Walker B, and ABC signature regions are displayed in red, blue, and yellow, respectively. The crystallographic structure is from the PDB file 1L7V (no nucleotide included; Locher et al., 2002). The vitamin B_{12} entry point is also shown in the figure.

Q-loop, and a histidine from the switch region (Schneider and Hunke, 1998; Locher et al., 2002). The Walker A motif of BtuCD is believed to play a role in the binding of the β- and γ-phosphates of the nucleotides (in analogy with the conserved aspartate in the Walker B motif of Av_2). The ABC signature sequence preceding the Walker B region is highly conserved in all ABC transporter family members and is a hallmark of the family. The residues in the Q-loop located at the interface of BtuC with BtuD are believed to be responsible for the interaction between the two domains, i.e., through them the mechanical force generated by ATP binding is transmitted from the ABC cassettes to the transmembrane domain (Locher et al., 2002).

ELASTIC NETWORK ANALYSIS

Elastic network model

The coarse-grained elastic network models, GNM and ANM, describe proteins as a network of masses (one per residue) with interactions between residues modeled using harmonic potentials with a single spring constant. The potential in ENM can be written in matrix notation as

$$V = V_0 + \frac{1}{2}\Delta\mathbf{R}^{\mathbf{t}}\underline{H}\Delta\mathbf{R}, \tag{1}$$

where V_0 is a constant (the potential at equilibrium) that does not affect the calculations. $\Delta\mathbf{R}$ in Eq. 1 represents a $3N$-dimensional vector in ANM and an N-dimensional vector in GNM. The superscript $\mathbf{t}$ denotes the matrix transpose. The Hessian matrix $\underline{H}$ contains the second derivatives of the potential V. Elastic network analysis, which is the same as normal mode analysis, requires diagonalization of the Hessian matrix by solving the secular equation

$$det[\underline{H} - \lambda\underline{I}] = 0. \tag{2}$$

Here, $\underline{I}$ is the identity matrix and λ is the eigenvalue.

The Hessian matrix elements in Eq. 1 for GNM are $H_{ii} = -\sum_{k\neq i}^{N} H_{ik}$ and $H_{ij}(i \neq j)$, which are given by

$$H_{ij} = \begin{cases} -\gamma & \text{for} \quad d_{ij} \le d_{ij}^0, \\ 0 & \text{for} \quad d_{ij} > d_{ij}^0, \end{cases} \tag{3}$$

where γ is the spring constant. Typically, γ is $\sim 1.0 \pm 0.5$ kcal/(mol Å^2) (Atilgan et al., 2002).

The ANM potential is

$$V = V_0 + \frac{1}{2}\gamma \sum_{i,j=1}^{N} (d_{ij} - d_{ij}^0)^2 h(d_{ij} - d_{ij}^0), \tag{4}$$

where d_{ij} is the distance between the i^{th} and the j^{th} nodes and the Heaviside function h is

$$h(d_{ij} - d_{ij}^0) = \begin{cases} 1 & \text{for} \quad d_{ij} \le d_{ij}^0 \\ 0 & \text{for} \quad d_{ij} > d_{ij}^0 \end{cases}. \tag{5}$$

Here, d_{ij}^0 is the cutoff distance beyond which no interactions between residues occur. Earlier studies (Atilgan et al., 2002) show that a short cutoff value yields extremely large-amplitude unphysical fluctuations. Typical cutoff values that reproduce crystallographic B-factors are 12–15 Å in the ANM model (Atilgan et al., 2002). In our ANM calculations, d_{ij}^0 is 15.0 Å for the nitrogenase Fe protein and $d_{ij}^0 = 12.0$Å for the BtuCD protein (a distance of 7 Å is used in our GNM computation for both proteins). Once the potential is defined, the Hessian matrix can be computed readily (Atilgan et al., 2002).

Correlation functions

Protein B-factors can be determined by x-ray crystallography. The mean-square (MS) fluctuation of the i^{th} residue, $\langle(\Delta\mathbf{R}_i)^2\rangle$, defines the B-factor

$$\langle(\Delta\mathbf{R}_i)^2\rangle = \frac{3}{8\pi^2}B_i, \tag{6}$$

where the MS fluctuations are

$$\langle(\Delta\mathbf{R}_i)^2\rangle = \frac{1}{Z_N}\int d\Delta\mathbf{R}(\Delta\mathbf{R}_i)^2 e^{-\beta V}. \tag{7}$$

Here $\beta = 1/k_BT$, k_B is Boltzmann's constant, T is the temperature, and $\Delta\mathbf{R}$ is a column vector consisting of $\Delta\mathbf{R}_1, \ldots, \Delta\mathbf{R}_N$. The constant Z_N is

$$Z_N = \int d\Delta\mathbf{R} e^{-\beta V}. \tag{8}$$

To describe the correlation of the fluctuations between residues, the orientational cross-correlations between the fluctuations of residues (coarse-grained to the C_α carbons) is

$$C(i,j) = \frac{\langle\Delta\mathbf{R}_i \cdot \Delta\mathbf{R}_j\rangle}{\{\langle(\Delta\mathbf{R}_i)^2\rangle\langle(\Delta\mathbf{R}_j)^2\rangle\}^{1/2}}, \tag{9}$$

where

$$\langle\Delta\mathbf{R}_i \cdot \Delta\mathbf{R}_j\rangle = \frac{1}{Z_N}\int d\Delta\mathbf{R} e^{-\beta V}\Delta\mathbf{R}_i\Delta\mathbf{R}_j. \tag{10}$$

In GNM, the cross-correlation function C_{ij} is expressed as a sum over M nonzero modes ($M = N-1$), given by Atilgan et al. (2001) as

$$\langle\Delta\mathbf{R}_i \cdot \Delta\mathbf{R}_j\rangle = \frac{3k_BT}{\gamma}\sum_{k=1}^{M} u_{ik}\frac{1}{\lambda_k}u_{kj}, \tag{11}$$

where λ_k is the eigenvalue of the k^{th} normal mode, and u_{ik} is the i^{th} component of the k^{th} eigenvector obtained by solving Eq. 2. The ANM cross-correlation function is the same as in Eq. 11, but $\Delta\mathbf{R}_i$ is replaced by its x, y, or z component and $M = 3N-6$. The analytical expression for the autocorrelation function in Eq. 7 is also obtained using Eq. 11 with $i = j$.

Both GNM and ANM provide useful tools to describe the global fluctuation dynamics of proteins around the native state. The major advantage of GNM is that it provides an accurate evaluation of protein fluctuations (B-factors) with a minimal computational cost. Whereas GNM is limited to the description of protein MS displacements and correlations between fluctuations, ANM can predict the directionality of protein conformational fluctuations.

RESULTS AND DISCUSSION

Nitrogenase Fe protein

To study the conformational motion of the Av_2 Fe protein, the crystallographic structure of the uncomplexed Av_2 at 2.15 Å resolution (Jang et al., 2000b) (PDB file 1Fe6P) was used. The B-factors (*solid line*) computed using GNM are compared with the experimental data (*dashed line*) in Fig. 3. The spring constant was 1.0 kcal/(mol Å^2) (Atilgan et al., 2002). As displayed in Fig. 3, the calculated results capture the main features of the experimental B-factors. The ANM approach was also employed in the calculations. No qualitative difference was found between the ANM and GNM results for the B-factors and the cross-correlations.

The large-scale conformational changes observed in the Fe-protein crystal structures involve the relative movement of large structural elements of the protein. To probe the features of this domain motion further, the cross-correlation matrix is plotted (Fig. 4). The cross-correlation function (defined in Eq. 9), is normalized so that it is unitless and bounded by ± 1. For the $+1$ value, the fluctuations of a residue pair are fully correlated. That is, the two residues move together. A cross-correlation of -1 means fully anti-correlated motion. Zero suggests uncorrelated movement.

The results shown in Fig. 4 identify two distinct regions in each of the two identical Av_2 subunits (denoted A and B in one subunit, and C and D in the other). The region A consists of residues 1–100, including α_1–α_3, β_1–β_4, the P-loop, and the Switch I region. The region B contains residues 101–286, incorporating Switch II, the P-loop, and the secondary structures α_4–α_9 and β_5–β_8. In this figure, the colors purple, blue, and yellow represent positive correlations ($C_{ij} > 0$), denoted by the plus signs in the circles, whereas green indicates the negatively correlated regions ($C_{ij} < 0$), labeled by the minus signs. The uncorrelated residue pairs ($C_{ij} = 0$) are colored brown. Fig. 4 shows the nature of the concerted motion. In each subunit, the intraunit fluctuations are positively correlated and indicate that the monomer moves collectively. The negative correlation of the two subunits indicates that the dimeric Fe protein can act as a molecular machine with two ''arms.''

The residue fluctuation-correlation patterns in the dimeric Fe protein are reflected in the motion of the GNM slowest mode, shown in Fig. 5. Here, the amplitude of the eigenvector in the lowest-frequency mode is plotted on the ordinate whereas the abscissa shows the residue number. The motion of the subunits (*AB* and *CD*) reflects the noncrystallographic symmetry (Strop et al., 2001) of the protein. Consistent with the cross-correlations indicated in Fig. 4, this mode shows that the residues in each subunit move together. In contrast, the

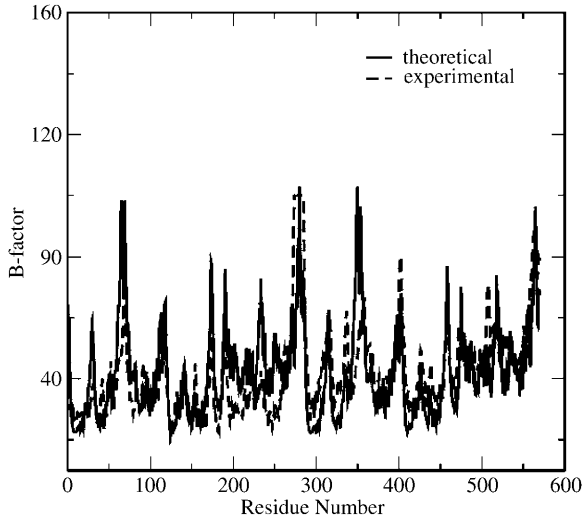

FIGURE 3 Computed and experimental B-factors of the nitrogenase Fe protein, Av_2, versus residue number. The GNM results are plotted in the solid line and the x-ray crystallographic data are shown with the dotted-dashed line.

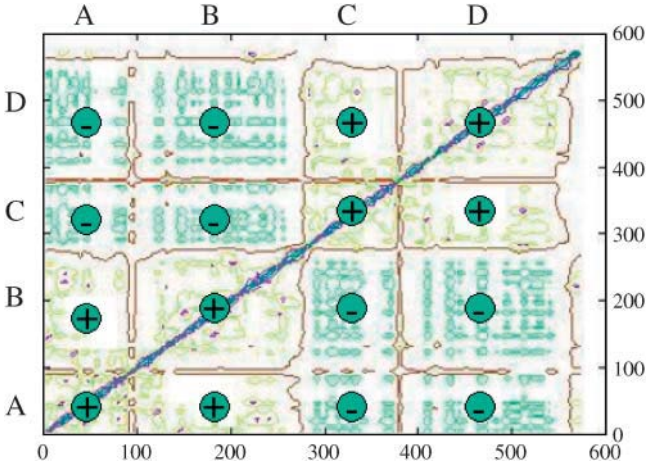

FIGURE 4 Contour plot of the cross-correlation function versus residue number for the nitrogenase Fe protein, Av_2. The colors purple, blue, and yellow indicate strongly correlated and correlated ($C_{ij} > 0$) regions, denoted by the plus signs in the circles. Green and brown refer to anticorrelated ($C_{ij} < 0$), labeled by the minus signs, and uncorrelated ($C_{ij} = 0$) residues pairs.

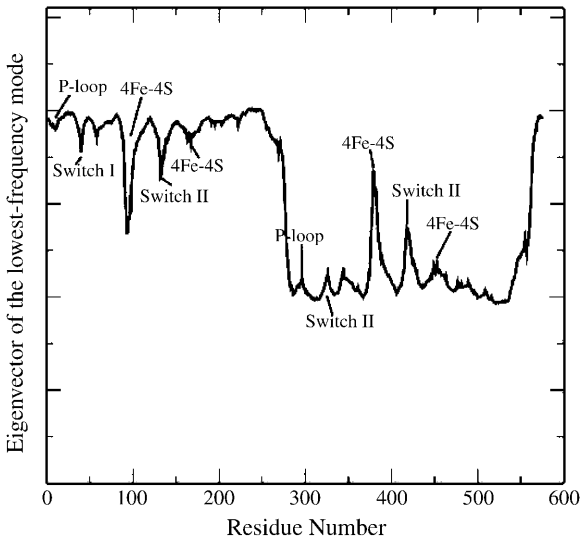

FIGURE 5 Eigenvector (defined in Eq. 9) of the slowest normal mode as a function of the residue number for the nitrogenase Fe protein, Av_2.

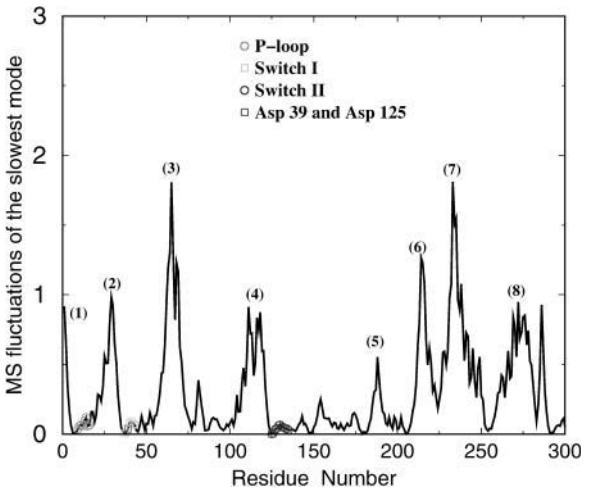

FIGURE 6 Residue mean-square fluctuations in the slowest mode of the nitrogenase Fe protein, Av_2. The amplitudes are normalized by that of residue 28. The P-loop, Switch I, Switch II, and two residues Asp^{125} and Asp^{39} are shown in the figure. The maxima are labeled, corresponding to the structures displayed in Fig. 7 *a*.

direction of the overall motions in different subunits is opposed. The residues involved in this lowest-frequency mode, seen from the figure, are associated with the nucleotide binding (P-loop), Switch I, Switch II, and the [4Fe4S] cluster.

We analyzed a series of low-frequency vibrational modes of the Fe-protein using both GNM and ANM. Only the slowest mode is found to undergo coherent and quasirigid body movements consistent with the pattern displayed in Fig. 4. This finding suggests that nitrogenase drives this mode to cause the collective motion via ATP binding that leads to Av_1 binding and energized electron transfer (Kurnikov et al., 2002).

Fig. 6 shows the residue MS fluctuations driven by the ANM slowest mode. The MS fluctuations of this mode display a symmetric pattern with respect to the twofold symmetry axis of the Fe protein. Here the data shown only for the first monomer (residues 1–287) are normalized by that of residue 28 for the convenience of plotting. The extrema displayed in this figure reflect the rigidity property of the protein. The maxima correspond to the flexible residues whereas the minima are associated with the stiff residues including the ''hinge'' sites. The significant peaks are labeled in the figure. As shown in Fig. 7 *a*, all these highly flexible residues are located on the surface of the protein. Among them, Glu^{59}–Leu^{70} (labeled *3*) at the interface that interacts with the MoFe protein are functionally associated with the protein-protein interaction.

High mechanical stability of residues located at the minima in Fig. 6 may be essential for the protein to execute large-scale conformational movements relevant to function. Important residues involved include the P-loop, Switch I, and Switch II. The corresponding structures are shown in Fig. 7 *b*. In this figure, the P-loop and Switch II are red ribbons and Switch I is represented by a red tube. Asp^{125}, Cys^{132} (both in Switch II), and Asp^{39} (in Switch I) are displayed with yellow lines. Switch II connects the P-loop through Asp^{125} (this residue may serve as a hinge) and interacts with the [4Fe4S] cluster via Cys^{132} (J. L. Schlessman et al., 1998; Jang et al., 2000b). These interactions are important for communication between the nucleotide-binding domain and the [4Fe4S] cluster (Jang et al., 2000b). Switch I extends the interactions with the P-loop through Asp^{39} to the region of residues 59–69 (labeled *3* in Fig. 6) which interact with the MoFe protein in the nitrogenase complex. As such, Switch I is believed to propagate the force generated from binding and hydrolysis of MgATP to the interface between the Fe protein and the MoFe protein (Jang et al., 2000b).

The residue MS fluctuations driven by the ANM slowest mode are also depicted in the ribbon diagram of Fig. 8. Flexibility increases in the color series red, green, and blue. The nucleotides and the [4Fe4S] cluster are shown with blue spheres. Asp^{125} and Asp^{39} are indicated with yellow lines.

Further ANM analysis demonstrates the directions of motion associated with the slowest mode (Fig. 8). The motion pattern displayed is also consistent with the GNM result, i.e., the two monomers move against each other whereas the intradomain movement is concerted. In other words, the residues driven by this global mode experience harmonic and cooperative motion.

BtuCD

The x-ray structure of BtuCD in the PDB file 1L7V (Locher et al., 2002) was used in our analysis. The sequence in this PDB file was rearranged so that the transmembrane domain is followed by the ATP-binding domain of the same subunit

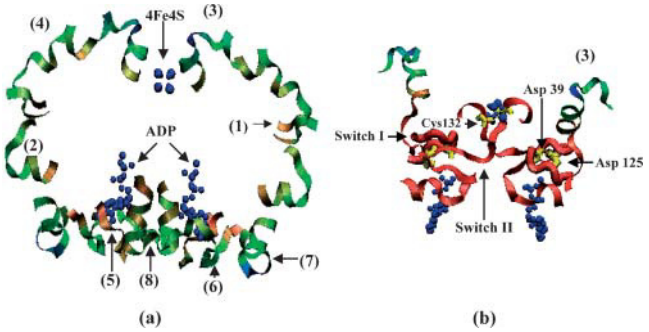

FIGURE 7 (*a*) Ribbon diagram of the residues located at the minima in Fig. 6, denoted by *1–10*. The ADP and the [4Fe4S] cluster are blue spheres. (*b*) Functionally important regions in the Av_2 protein. Switch II and the P-loop are depicted in red ribbons, Switch I is plotted in red tube, and Asp^{125}, Asp^{39}, and Cys^{32} are yellow bonds. The residue regions corresponding to *3* in *a* are also shown.

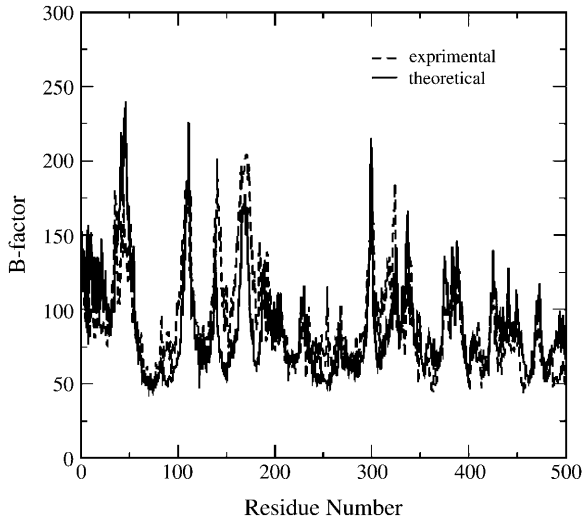

FIGURE 9 Computed and experimental B-factors of the BtuCD protein versus residue number. The ENM results are plotted with the solid line and the experimental values are shown with the dotted-dashed line (only the *A* subunit—transmembrane domain in BtuC—and *B* subunit—ATP-binding domain in BtuD—are shown in this figure).

for the convenience of analysis. The GNM-calculated B factors (*solid line*) compared with those from the experiments (*dashed curve*) are shown in Fig. 9. The calculations are in agreement with the experiments.

The cross-correlation functions computed using the GNM method for BtuCD are shown in Fig. 10. As with those of Fig. 4, the colors purple, blue, and yellow refer to positively correlated regions ($C_{ij} > 0$), denoted by the plus signs in the circles. The green regions correspond to the negatively correlated residue pairs ($C_{ij} < 0$, labeled with *minus signs*). The color brown indicates the uncorrelated residues ($C_{ij} = 0$). The four distinct regions of motion are associated with two transmembrane domains (denoted *A* and *C*) and two ABC units (denoted *B* and *D*). The correlations between *A* and *C*, and between *B* and *D*, are fairly weak. Nevertheless, a concerted correlation pattern—similar to that seen in the nitrogenase Fe protein—is observed. That is, in each subunit, the residue motion is positively correlated whereas the intersubunit motion is negative or weakly correlated. This means that the two subunits of the BtuCD dimer move against each other in concert as semirigid bodies. Also, as with the nitrogenase Fe protein, the lowest-frequency mode captures this highly cooperative feature of the dimer, depicted in Fig. 11. This mode also correlates all important functional regions, including the Walker A (nucleotide-binding region) and Walker B regions, as well as the important transmembrane helices.

The ANM-computed MS fluctuations (normalized by that of residue 165) of the slowest mode are shown in Fig. 12. The membrane residues of TM1–TM10 are all at the minima in the figure, reflecting their stiffness as presumably related to function. The P-loop and Walker B regions are also indicated in the figure. The L-loop residing between TM6 and TM7 forms the interface between the transmembrane domain and the ABC cassette. The L-loop is of functional importance in transmitting the force generated from the nucleotide binding and hydrolysis to the transmembrane domain. The maxima in Fig. 12 correspond to the residue regions located on the protein surface. A side view (parallel to the membrane bilayer) of the protein structure, colored according to the residue MS fluctuation amplitude in the lowest-frequency mode, is shown in Fig. 13. The colors in order of increasing flexibility are red, green, and blue. The residues outside the membrane are relatively flexible, serving as recognition sites to bind the periplasmic binding protein of B_{12}, BtuF (Locher et al., 2002). The concerted manner to open the transport pathway coupled to the lowest-frequency mode is shown in Fig. 13 *b*, evaluated with ANM. As with the nitrogenase Fe protein, the ANM-predicted directions of motion are consistent with the cross-correlated patterns computed with GNM.

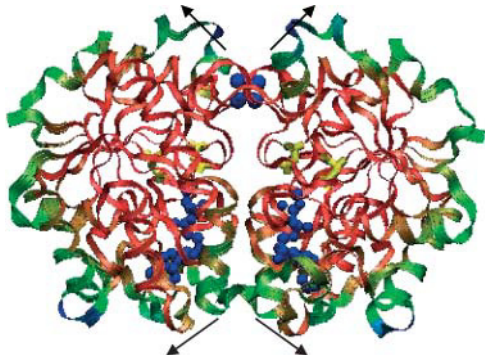

FIGURE 8 Ribbon diagram of the Av_2 protein. The amplitudes of the residue MS fluctuations of the slowest mode increase as colors vary from red, green, and blue. The ADP and the [4Fe4S] cluster are shown in blue spheres. The motion directions of the slowest mode are also shown, corresponding to the pathway opening.

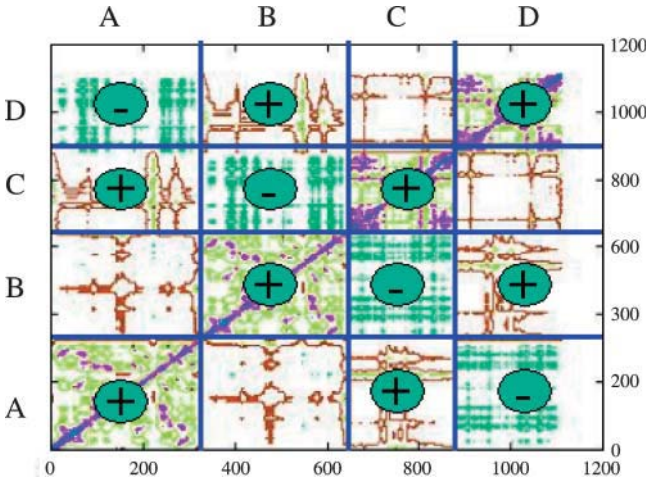

FIGURE 10 Contour plot of the cross-correlation function versus residue number for the BtuCD protein. The regions colored purple, blue, and yellow refer to strongly correlated and correlated ($C_{ij} > 0$), denoted by the plus signs in the circles. The colors green and brown indicate the anticorrelated ($C_{ij} < 0$), labeled by the minus signs, and uncorrelated ($C_{ij} = 0$) residue pairs.

CONCLUDING REMARKS

Large-scale conformational changes of nucleotide-utilizing proteins play a critical role in protein function. The free-energy transduction from ATP is focused or hinged on the [4Fe4S] cluster in the case of the nitrogenase Fe-protein, and the gating region of the B_{12} transport pathway in the BtuCD case.

Elastic network analysis provides insights into the mechanism of high-efficiency energy transduction over large distances. The ENM calculations indicate that these two proteins can act as semirigid lever arms to generate concerted large-scale conformational changes. Further evidence from the ENM investigation illustrates that this collective motion is dominated by the lowest-frequency normal mode. As such, we suggest that ATP binding and hydrolysis drives the motion of this mode, resulting in large-scale conformational changes to the proteins.

The elastic network analysis used above is closely related to the normal-mode analysis widely employed in the literature (e.g., Li and Cui, 2002, 2004), within a coarse-grained description. Our calculations indicate that elastic network analysis is a useful tool to analyze a large-scale conformational motion in large proteins. The nature of the biological processes driven by ATP binding and hydrolysis is, of course, highly anharmonic. These processes involve the transition between different chemical states. The crystal structures associated with these ATP- and ADP-bound states, for example, are available for the nitrogenase proteins (Jang et al., 2000a,b). The above elastic network model can

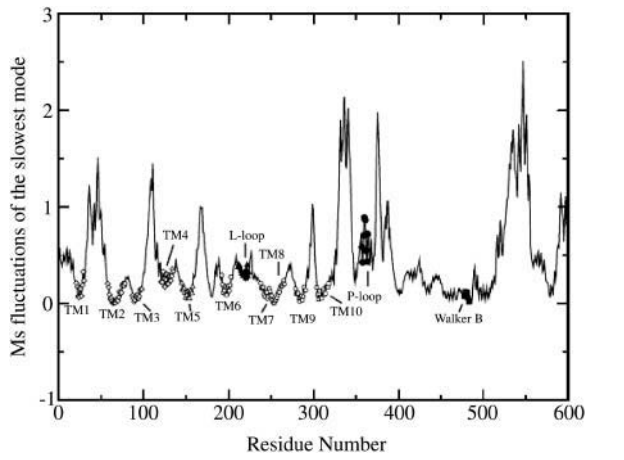

FIGURE 12 Residue mean-square fluctuations in the slowest mode of the BtuCD protein. The amplitudes are normalized by that of residue 165. The transmembrane helices *TM1–TM10*, L-loop, P-loop, and Walker B are shown in the figure.

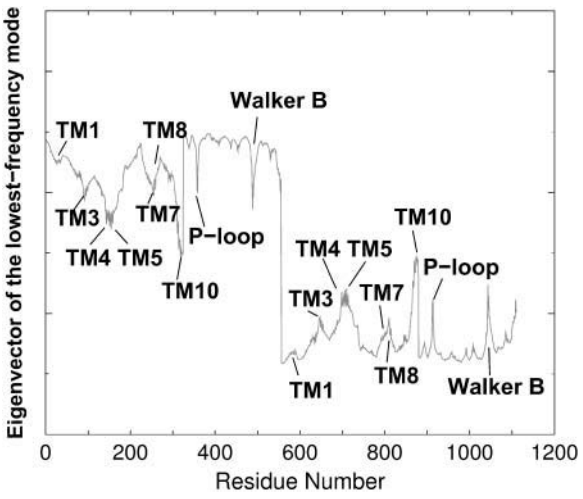

FIGURE 11 Eigenvector of the lowest-frequency normal mode as a function of the residue number for the ABC transporter, BtuCD.

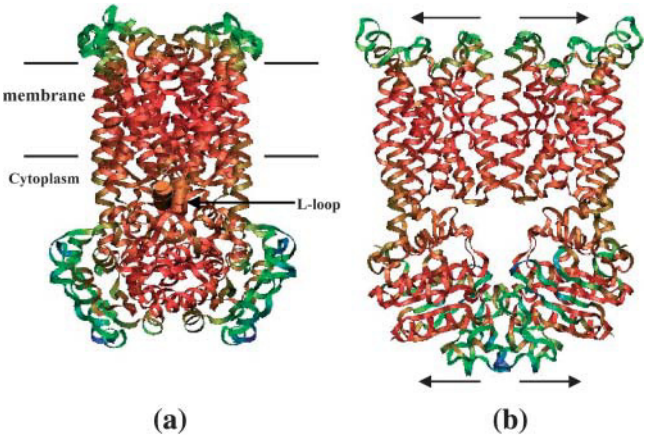

FIGURE 13 Ribbon diagram of the residue MS fluctuations driven by the slowest mode of the BtuCD protein. In the order of increasing the flexibility, the colors are red, green, and blue. (*a*) The side view of the protein parallel to the membrane bilayer and (*b*) the directions of the slowest mode motion, corresponding to the transporter-pathway opening.

be applied to these endpoint protein conformations and interpolated structures. Work along this line remains in the future.

We are grateful to the Bahar group for helpful discussion.

This work was supported by the National Institutes of Health (GM57876) and Duke University.

REFERENCES

Atilgan, A. R., S. R. Durell, R. L. Jernigan, M. C. Demirel, O. Keskin, and I. Bahar. 2002. Anisotropy of fluctuation dynamics of proteins with an elastic network model. *Biophys. J.* 80:505–515.

Bahar, I. A., R. Atilgan, M. C. Demirel, and B. Erman. 1997. Vibrational dynamics of folded proteins. Significance of slow and fast modes in relation to function and stability. *Phys. Rev. Lett.* 80:2733–2736.

Bahar, I., R. Atilgan, and B. Erman. 1997. Direct evaluation of thermal fluctuations in protein using a single parameter harmonic potential. *Folding Des.* 2:173–181.

Bahar, I., B. Erman, R. L. Jernigan, A. R. Atilgan, and D. Covell. 1999. Collective motions of HIV-1 reverse transcriptase. Examination of flexibility and enzyme function. *J. Mol. Biol.* 285:1023–1037.

Chang, G., and C. B. Roth. 2001. Structure of MsbA from *E. coli*: a homolog of the multidrug resistance ATP binding cassette (ABC) transporters. *Science.* 293:1793–1800.

Cramer, W. A., and D. B. Knaff. 1989. Energy Transduction in Biological Membranes. Spring-Verlag, New York.

Doruker, P., A. R. Atilgan, and I. Bahar. 2000. Dynamics of proteins predicted by molecular dynamics simulations and analytical approaches: application to a-amylase inhibitor. *Proteins Struct. Funct. Gen.* 40: 512–524.

Eady, R. R. 1996. Structure-function relationships of alternative nitrogenases. *Chem. Rev.* 96:3013–3030.

Einsle, O., F. A. Tezcan, S. L. A. Andrade, B. Schmid, M. Yoshida, J. B. Howard, and D. C. Rees. 2002. Nitrogenase MoFe-protein at 1.16 Å resolution: a central ligand in the FeMo-cofactor. *Science.* 297:1696–1700.

Hill, T. L. 1977. Free Energy Transduction in Biology: The Steady-State Kinetic and Thermodynamic Formalism. Academic Press, New York.

Howard, J. B., and D. C. Rees. 1996. Structural basis of biological nitrogen fixation. *Chem. Rev.* 96:2965–2982.

Hung, L. W., I. X. Wang, K. Nikaido, P.-Q. Liu, G. F.-L. Ames, and S.-H. Kim. 1998. Crystal structure of the ATP-binding subunit of an ABC transporter. *Nature.* 396:703–707.

Isin, B., P. Doruker, and I. Bahar. 2002. Functional motions of influenza virus hemagglutinin: a structure-based analytical approach. *Biophys. J.* 82:569–581.

Jang, S. B., L. C. Seefeldt, and J. W. Peters. 2000a. Modulating the midpoint potential of the [4Fe-4S] cluster of the nitrogenase Fe protein. *Biochemistry.* 39:641–648.

Jang, S. B., L. C. Seefeldt, and J. W. Peters. 2000b. Insights into nucleotide signal transduction in nitrogenase: structure of an iron protein with MgADP bound. *Biochemistry.* 39:14745–14752.

Jones, P. M., and A. M. George. 2002. Mechanism of ABC transporters: a molecular dynamics simulation of a well-characterized nucleotide-binding subunit. *Proc. Natl. Acad. Sci. USA.* 99:12639–12644.

Karplus, M., and J. A. McCammon. 2002. Molecular dynamics simulations of biomolecules. *Nat. Struct. Biol.* 9:646–652.

Keskin, O., S. R. Durell, I. Bahar, R. L. Jernigan, and D. G. Covell. 2002. Relating molecular flexibility to function: a case study of tubulin. *Biophys. J.* 83:663–680.

Keskin, O., R. L. Jernigan, and I. Bahar. 2000. Proteins with similar architecture exhibit similar large-scale dynamic behavior. Specificity resides in local differences. *Biophys. J.* 78:2093–2106.

Kurnikov, I. V., A. K. Charnley, and D. N. Beratan. 2002. From ATP to electron transfer: electrostatics and free-energy transduction in nitrogenase. *J. Phys. Chem. B.* 105:5359–5367.

Li, G., and Q. Cui. 2002. A coarse-grained normal mode approach for macromolecules: an efficient implementation and application to Ca^{2+}-ATPase. *Biophys. J.* 83:2457–2474.

Li, G., and Q. Cui. 2004. Analysis of functional motions in Brownian molecular machines with an efficient block mode approach: myosin-II and Ca^{2+}-ATPase. *Biophys. J.* 86:743–763.

Locher, K. P., A. T. Lee, and D. C. Rees. 2002. The *E. coli* BtuCD structure: a framework for ABC transporter architecture and mechanism. *Science.* 296:1091–1098.

Mogilner, A., H. Wang, T. Elston, and G. Oster. 2002. Molecular motors: theory and experiment. *In* Computational Cell Biology. C. Fall, E. Marland, J. Wagner, and J. Tyson, editors. Springer-Verlag, New York.

Rosenberg, M. F., Q. Mao, A. Holzenburg, R. C. Ford, R. G. Deeley, and S. P. C. Cole. 2001. Mutation of a single conserved tryptophan in multidrug resistance protein 1 (MRP1/ABCC1) results in loss of drug resistance and selective loss of organic anion transport. *J. Biol. Chem.* 276:15616–15624.

Schindelin, H., C. Kisker, J. L. Schlessman, J. B. Howard, and D. C. Rees. 1992. Structure of $ADP.AlF^{-}_{4}$-stabilized nitrogenase complex and its implications for signal transduction. *Nature.* 386:370–376.

Schlesinger, W. H. 1991. Biogeochemistry: An Analysis of Global Change. Academic Press, San Diego, CA.

Schlessman, J. L., D. Woo, L. Joshua-Tor, J. B. Howard, and D. C. Rees. 1998. Conformational variability in structures of the nitrogenase iron protein from *Azotobacter vinelandii* and *Clostridium pasteurianum*. *J. Mol. Biol.* 280:669–685.

Schneider, E., and S. Hunke. 1998. ATP-binding-cassette (ABC) transport systems: functional and structural aspects of the ATP-hydrolyzing subunits/domains. *FEMS Microbiol. Rev.* 22:1–20.

Stephens, P. J., D. R. Jollie, and A. Warshel. 1996. Protein control of redox potentials of iron-sulfur proteins. *Chem. Rev.* 96:2491–2514.

Strop, P., M. T. Patricia, H.-J. Chiu, H. C. Angove, B. K. Burgess, and D. C. Rees. 2001. Crystal structure of the all-ferrous $[4Fe\text{–}4S]^{0}$ form of the nitrogenase iron protein from *Azotobacter vinlandii*. *Biochemistry.* 40:651–656.

Tama, F., and Y.-H. Sanejouand. 2001. Conformational change of protein arising from normal mode calculations. *Protein Eng.* 14:1–6.

Tirion, M. M. 1996. Large amplitude elastic motions in proteins from a single-parameter, atomic analysis. *Phys. Rev. Lett.* 77:1905–1908.

World Health Organization. Geneva, Switzerland. 2000. Drug resistance to reverse medical progress. *WHO Press Rel.* 41.

Xu, C., D. Tobi, and I. Bahar. 2003. Allosteric changes in protein structure computed by a simple mechanical model: hemoglobin $T \leftrightarrow R2$ transition. *J. Mol. Biol.* 333:153–168.

Yuan, Y.-R., S. Blecker, O. Martsinkevich, L. Millen, P. J. Thomas, and J. F. Hunt. 2001. The crystal structure of the MJ0796 ATP-binding cassette. Implications for the structural consequences of ATP hydrolysis in the active site of an ABC transporter. *J. Biol. Chem.* 276:32313–32321.